JOURNAL OF CATALYSIS 86, 315–327 (1984)

Ethane Hydrogenolysis and Carbon Monoxide Hydrogenation over Niobia-Supported Nickel Catalysts: A Hierarchy to Rank Strong Metal–Support Interaction

E. I. Ko,[1] J. M. Hupp, and N. J. Wagner

Department of Chemical Engineering, Carnegie-Mellon University, Pittsburgh, Pennsylvania 15213

Received August 4, 1983; revised October 23, 1983

Ethane hydrogenolysis and carbon monoxide hydrogenation were studied over two niobia (Nb_2O_5)-supported nickel catalysts, containing 2 and 10 wt% nickel, which had been reduced in hydrogen at 573 or 773 K for 1 h. Compared to silica-supported nickel catalysts, these samples had lower ethane hydrogenolysis activity but higher CO hydrogenation activity. For some samples a different experimental rate law for ethane hydrogenolysis was observed. In CO hydrogenation, all samples showed a shift in product distribution to hydrocarbons higher than methane, and olefinic products were detected. These observations were attributed to strong metal–support interaction (SMSI). The use of these chemical probes identified different manifestations of SMSI that depend on crystallite size and reduction treatment. On the basis of these manifestations, a hierarchy consisting of five stages was developed to rank the extent of interaction in Ni/Nb_2O_5 catalysts. A mechanism of SMSI was proposed for a physical explanation of this hierarchy.

INTRODUCTION

In a previous paper (*1*), we reported on the reduction and chemisorption behavior of niobia-supported nickel catalysts as part of our study regarding strong metal–support interaction (SMSI) (*2*). Our results identify crystallite size, reduction treatment, and support reducibility as some of the critical parameters in a SMSI system. A niobia-supported nickel catalyst, properly pretreated, chemisorbs significantly less hydrogen at room temperature compared to a silica-supported nickel catalyst.

In addition to a suppression in hydrogen chemisorption, a niobia-supported nickel catalyst has unusual activity and selectivity in CO hydrogenation, as described elsewhere (*3*). These earlier results are for a 10 wt% Ni/Nb_2O_5 sample reduced at 773 K for 1 h. Since then, we have expanded the work to examine the effects of the critical parameters of SMSI on reaction activity and selectivity. We have also included ethane hydrogenolysis as another probe reaction. The Ni/Nb_2O_5 catalysts were found to behave very differently with respect to these two probe reactions.

Ethane hydrogenolysis and CO hydrogenation have been used as chemical probes by many investigators on a large number of SMSI catalysts over the past few years. Ko and Garten (*4*) studied ethane hydrogenolysis over group VIII metals supported on TiO_2. Haller and co-workers (*5*, *6*) have examined the same reaction on titania-supported Rh and Rh–Ag bimetallic catalysts. Recently, results specifically for titania-supported nickel have been reported by Ko *et al.* (*7*) and Burch and Flambard (*8*, *9*). Results of SMSI catalysts in CO hydrogenation are even more extensive. Nickel, in particular, has been examined in many studies as supported-metal catalysts (*8–14*) and model support systems (*15–17*). Other metals that have been studied include platinum (*18*), palladium (*19*, *20*), and ruthenium (*21*).

[1] To whom all correspondence should be addressed.

0021-9517/84 $3.00

Despite the extensive literature, many questions remain unanswered concerning these two reactions over SMSI catalysts. For example, it is equivocal whether nickel has a lower ethane hydrogenolysis activity when supported on titania compared to silica (*4, 9*). In the case of CO hydrogenation, most authors agree that the activity and selectivity are different on a titania-supported catalyst. However, the controversy centers on the nature of active sites (*8, 14*), or the nature of the interaction itself (*13*).

In our study of these two reactions over niobia-supported nickel catalysts, we were able to identify different stages of strong metal–support interaction by a systematic variation of several key parameters. The purpose of this paper is to present these new kinetic results and in so doing, develop a hierarchy system to rank the extent of SMSI. This hierarchy will be used to critically examine current literature data, and to shed some light on the SMSI mechanism.

EXPERIMENTAL

Catalyst Preparation

The preparation of niobia-supported nickel catalysts were reported in detail elsewhere (*1*). Briefly, the niobia support was prepared in a manner similar to that described by Tauster and Fung (*22*). This procedure consists of titrating a methanolic solution of niobium(V) chloride with ammonium hydroxide. The resultant precipitate is filtered, washed, and calcined in oxygen to give a crystalline Nb_2O_5 phase. The particular support used in this study was calcined for 2 h at 773 K and had a BET surface area of about 10 m^2/g. Two catalysts, containing 2 and 10 wt% nickel, were prepared by the incipient wetness impregnation of niobia with an aqueous solution of nickel nitrate hexahydrate. The weight loadings were confirmed by atomic absorption measurements. Prior to kinetic studies, the catalysts were heated in flowing hydrogen (3 liters/h) at a rate of 10–15 K/min to the desired reduction temperature, and held at that temperature for 1 h. The average crystallite sizes of the reduced samples, measured by X-ray line broadening technique, were found to be 4 and 9 nm for the 2 and 10 wt% catalysts, respectively. As shown previously (*1*), the difference in crystallite size accounts for the effect of metal loading on the SMSI behavior of these catalysts.

Microreactor System

The kinetic measurements were carried out in a microreactor system. The gases used were helium (Airco, 99.999% purity), hydrogen (Airco, 99.999% purity), ethane (Matheson, 99.96% purity), hydrogen/CO mixture (Airco, 25% CO), and nitrogen (Airco, 99.999% purity). Hydrogen was further purified through a DEOXO purifier (Englehard) and through a molecular sieve trap (Union Carbide, Linde 5A). The remaining gases, except ethane, were passed through a molecular sieve trap. Ethane was used directly as supplied. The flow rates of the various gases were monitored by pressure transducers (Microswitch, Model 142PC 15D), which had been calibrated individually for each gas.

The reactor consisted of a stainless-steel tube, 17 cm long and 1.5 cm OD. To hold the catalyst, a stainless-steel disk and disk support were fitted 1.5 cm from the open end of the tube. The amount of sample used in a typical run was about 300 mg. A chromel–constantan termocouple (Omegaclad) imbedded in the disk recorded the bed temperature. Heating of the reactor was done by a cylindrical ceramic heating furnace which encircled the reactor. The furnace was controlled by a Variac and a temperature controller (Nanmac Corp., PC-1) in series. The reactor outlet is connected to an on-line gas chromatagraph (Perkin–Elmer Sigma 2B) for product analysis. The various species were separated by a Chromosorb 102 column, and their relative amounts determined by a thermal conductivity detector. The responses of the detector were directly analyzed by an integrator

(Hewlett–Packard, 3390A). The exact procedure for the GC analysis, including calibrations, temperature programming schedules and calculations, are described elsewhere (*23*).

Ethane Hydrogenolysis

The reaction of ethane hydrogenolysis was run at a total pressure of 1 atm with the reactor operated in a differential mode. The reactant gases, ethane and hydrogen, were mixed in a helium carrier stream before entering the reactor. The total flow rate was 18 liters/h, while the flow rates of ethane and hydrogen were varied in order to obtain different partial pressures. In a typical run, a catalyst sample of approximately 300 mg was loaded into the reactor and reduced, as described previously. After reduction, the catalyst was cooled to the reaction temperature in helium at a flow rate of 3 liters/h. It was then exposed to the reactant gases for 3 min whereupon an effluent gas sample was taken for GC analysis. Between runs, the ethane flow rate was cut off while hydrogen and helium continued to flow through the reactor for 10 min.

The above procedure was similar to that used by Yates *et al.* (*24*). Their "bracketing-technique" was also followed in this study to determine exponents n and m in the exponential rate law;

$$\text{rate} = kp_E{}^n p_H{}^m$$

where p_E and p_H represent the partial pressures of ethane and hydrogen, respectively. In this approach, a run at a given set of partial pressures is bracketed by runs at a standard set of conditions (p_E = 0.03 atm, p_H = 0.2 atm). The values of m and n were then determined by comparing the rate at a given set of partial pressures with the average rate of the two standard sets that bracketed it. This procedure minimized any variation in catalytic activity. The activation energy was determined by studying the effect of temperature on the reaction rate with the partial pressures of the reactants held at the standard conditions, and analyzing the results in a typical Arrhenius plot.

Carbon Monoxide Hydrogenation

All CO/H_2 kinetic experiments in this study were operated at a total pressure of 1 atm, a CO/H_2 ratio of 1/3, a total flow rate of between 0.5 and 1.8 liters/h, and a reaction temperature between 450 and 510 K. The conversion of CO was always kept to a few percents to ensure a differential operation. The procedure used was similar to that suggested by Vannice (*25*). After an *in situ* reduction, the catalyst was cooled in hydrogen (3 liters/h) to the reaction temperature. After the temperature had stabilized, the feed gas was sent through the catalyst bed for 20 min, typically at 1.2 liters/h. A sample of the product gas mixture was then taken for GC analysis. Next, the feed gas was replaced by a 20-min hydrogen purge (3 liters/h) that regenerated the catalyst. During this time, the reactor temperature was reset to a new value for the next run. Reactant flow rates lower and higher than the standard 1.2 liters/h were also used to examine the dependence of conversion and product distribution on flow rate.

Conversion and activation energy of the reaction were calculated in terms of both the consumption of carbon monoxide and the formation of methane. Hydrocarbon products up to C_5 were monitored, and their distribution was expressed in mole percent. The emphasis of this study was on the hydrocarbon products, especially the olefin/paraffin ratios, so CO_2 and H_2O were not included in this calculation. For this reason, the mole percentages of all hydrocarbons (up to C_5) summed to 100.

RESULTS

Ethane Hydrogenolysis

The kinetic results for ethane hydrogenolysis over Ni/Nb_2O_5 catalysts are summarized in Table 1. The notation (i, j, k), where i = metal loading, in wt%, j = reduction temperature, in K, and k = reduction

TABLE 1

Kinetic Results for Ethane Hydrogenolysis over Ni/Nb_2O_5 Catalysts

Catalyst and treatment	E_A [a] (kJ/mole)	r_0' [b] (molecules/s/surface Ni atom)	n [c]	m [c]	Activity at 478 K (molecules/s/surface Ni atom)
(2,573,1)	176	1.74×10^{13}	1.1	−1.1	1.1×10^{-6}
(2,773,1)	180	5.36×10^{12}	1.0	−1.2	1.2×10^{-7}
(10,573,1)	183	4.72×10^{14}	0.9	−1.7	4.9×10^{-6}
(10,773,1)	170	4.96×10^{11}	1.0	−0.9	1.4×10^{-7}
(10,573,1, 773,1-N_2) [d]	173	9.43×10^{12}	0.9	−1.6	1.2×10^{-6}
(10,573,1, 773,1-He) [d]	179	7.19×10^{12}	0.9	−0.8	2.0×10^{-7}

[a] Determined from the temperature dependence of the rate r_0, at ethane and hydrogen partial pressure of 0.03 and 0.2 atm, respectively.

[b] Preexponential factor in the equation $r_0 = r_0' \exp(-E_A/RT)$.

[c] Exponents in the experimental power rate law, $kp_E^n p_H^m$.

[d] Experiments in which the catalyst was heated in an inert gas. See text for explanation.

time at j K in h, will be used throughout this paper to denote the catalyst and pretreatment. Our previous results (*1*) show that catalysts in this study were completely reduced under the pretreatments used. The activity is expressed in molecules of ethane reacted/s/surface Ni atom (molecules/s/Ni). The usual procedure of using hydrogen chemisorption data to determine the number of surface atoms is inappropriate here, since these SMSI catalysts show the characteristic suppression of hydrogen chemisorption (*1*). Instead, the number of surface sites is calculated from the average crystallite size, measured by X-ray diffraction. This approach implicitly assumes that all surface sites are active, which may or may not be true. However, such a calculation will lead to a meaningful comparison of the relative activity between catalysts. The activity data for both ethane hydrogenolysis and CO hydrogenation in this paper are thus calculated on the same basis. All Ni/Nb_2O_5 catalysts in this study showed a lower activity for ethane hydrogenolysis than bulk nickel or nickel supported on a noninteracting support. As summarized by Burch and Flambard (*9*), the activities of the latter materials range from 2.4 to 7.6×10^{-4} molecules/s/Ni measured in the range of 473–478 K. Using a set of experimental conditions very similar to our own, Taylor *et al.* (*26*) reported an activity range of 10^{-2}–10^{-4} molecules/s/Ni at 478 K for Ni/SiO_2 catalysts containing 1, 5, and 10 wt%. In order to compare our results with these literature values, we have included the activities for Ni/Nb_2O_5 catalysts at 478 K in Table 1. The low activities of these catalysts necessitated running the reaction at temperatures higher than 478 K. The calculation of activities at 478 K thus involved extrapolation of activity data with the experimentally determined activation energy. A comparison of activity at any other temperature is straightforward.

It should be noted from Table 1 that although all catalysts underwent a suppression in ethane hydrogenolysis activity, the extent of suppression differed. After a 573 K reduction for 1 h, the 2 wt% sample was about a factor of 5 less active than the 10 wt% sample. Both samples exhibited a further decline in activity as the reduction temperature was raised from 573 to 773 K.

In addition to a change in activity, the experimental rate law measured for these Ni/Nb_2O_5 catalysts are different than that

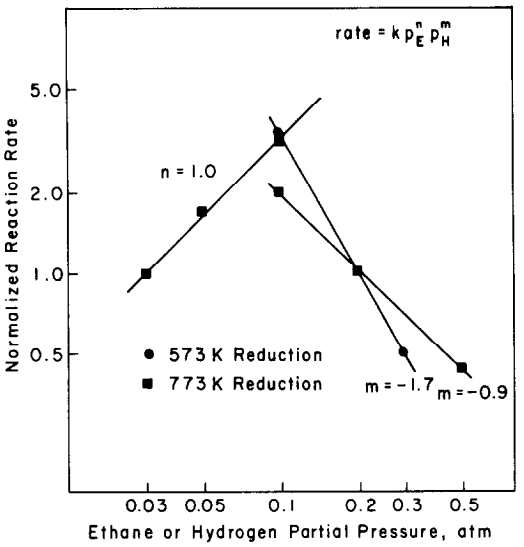

FIG. 1. Determination of the experimental rate law of ethane hydrogenolysis for a 10 wt% Ni/Nb_2O_5 catalyst: (●) reduced at 573 K for 1 h, (■) reduced at 773 K for 1 h. The ethane partial pressure dependence is only shown for the (10,773,1) sample as there is little difference between the two reduction temperatures.

found for Ni/SiO_2 catalysts. The extensive work of Sinfelt and co-workers (*26, 27*) showed that for Ni/SiO_2 catalysts, the ethane partial pressure dependence (n) is approximately +1 and the hydrogen partial pressure dependence (m) is approximately −2. In this study the value of n was found to be in the range 0.9–1.1, similar to that of Ni/SiO_2 catalysts. On the other hand, a much weaker hydrogen partial pressure dependence was found for some of the catalysts. The value of m is about −1 for the 2 wt% sample after reduction at both 573 and 773 K. For the 10 wt% sample, m had a value of −1.7 after a 573 K reduction, but increased to −0.9 when the reduction temperature was raised to 773 K. Such a change is illustrated in Fig. 1.

In a previous paper (*1*), we reported that further heating of a (10, 573, 1) sample in an inert gas to 773 K changes the chemisorption behavior, and that the effect is different between nitrogen and helium. For comparison, identical treatments were used in this study, and the results are presented as the last two enteries in Table 1. It was found that the activity of ethane hydrogenolysis dropped after heating in either nitrogen or helium to 773 K for 1 h, with a larger drop observed for the latter. In fact, the activity of the (10,573,1,773,1-He) sample was comparable to that of a (10,773,1). Concurrent with the drop in activity, the (10,573,1,773,1-He) sample also had a value of m of −0.8. This is to be contrasted with the (10,573,1,773,1-N_2) sample, which maintained approximately the same values of n and m as those for (10,573,1) and also had a less severe drop in activity.

CO Hydrogenation

The activity and selectivity of all catalysts in this work were studied as a function of temperature and flow rate. The temperature variation was used to obtain the activation energy. The flow rate variation enabled the conversion to be changed at a constant temperature so that the effect on product distribution could be observed. Table 2 lists a typical series of runs for the (10,773,1) sample. The first notable result is that the catalyst produced a large amount of hydrocarbons other than methane. Ni/SiO_2 catalysts, by comparison, produce primarily methane (*10, 12*). Perhaps even more intriguing was the fact that of these higher hydrocarbon products, a large fraction were olefins. The olefin/paraffin ratio was particularly large for C_3 and C_4 hydrocarbons.

The product distribution shown in Table 2 is very similar to those for other Ni/Nb_2O_5 catalysts, in that the two characteristics of a lower methane yield and high olefin/paraffin ratios were always observed. Instead of presenting all product distributions, we chose to compare these catalysts in terms of their kinetic parameters. Shown in Table 3 are activation energies and turnover frequencies, expressed in terms of both CO conversion and methane formation, for the various samples. The turnover frequencies were calculated for 548 K to allow a direct

TABLE 2

Product Distribution for a 10 wt% Ni/Nb_2O_5 Catalyst Reduced at 773 K for 1 h

Temperature (K)	Flow rate (l/h)	CO conversion (%)	Hydrocarbon distribution (mole %)					Olefin/paraffin ratio		
			C_1	C_2	C_3	C_4	C_5	C_2	C_3	C_4
476	1.2	2.2	43.8	32.7	12.1	5.91	5.52	0.05	0.55	1.30
476	1.8	1.0	51.6	37.0	9.37	2.06	—	0.06	0.44	1.20
476	0.8	3.1	47.1	33.5	14.6	3.14	1.59	0.05	0.46	0.60
484	1.2	2.4	51.0	31.0	14.7	3.00	0.30	0.02	0.55	1.45
489	1.2	4.0	52.9	28.6	13.7	4.54	0.27	0.02	0.32	0.48
489	1.8	2.5	51.4	30.1	14.1	3.13	1.25	0.06	0.56	0.94
489	0.5	7.7	51.8	27.5	14.3	6.30	0.09	0.01	0.16	0.45
500	1.2	5.9	55.2	24.9	13.9	4.94	1.04	0.02	0.23	0.22

comparison with literature values. At the same temperature, the activity for Ni/SiO_2 catalysts in CO hydrogenation is in the range of 0.5–1.5 $\times$ 10^{-2} s^{-1} (*9*). Bartholomew *et al.* (*12*) studied several Ni catalysts covering a wide crystallite size range, and reported turnover numbers which vary between 1.3 and 4.9 $\times$ 10^{-3} s^{-1} at 525 K in terms of methane, and 1.7–5 $\times$ 10^{-3} s^{-1} in terms of CO. Extrapolation of our data to 525 K gives corresponding values of 3.3–7.6 $\times$ 10^{-3} and 0.9–2.0 $\times$ 10^{-2} s^{-1}. It thus appears that the CO hydrogenation activity of Ni/Nb_2O_5 catalysts is comparable to, or even better than that of Ni/SiO_2 catalysts.

TABLE 3

Kinetic Results for CO Hydrogenation over Ni/Nb_2O_5 Catalysts

Catalyst and treatment	Activation energy (kJ/mole)		Turnover frequency at 548 K ($\times$ 10^{-2} s^{-1})	
	E_{CH_4}	E_{CO}	N_{CH_4}	N_{CO}
(2,573,1)	112	112	1.9	4.2
(2,773,1)	128	99	2.6	3.5
(10,573,1)	123	123	2.4	6.3
(10,773,1)	116	112	1.8	5.8
(10,573,1,773,1-N_2)[a]	126	101	1.1	2.3
(10,573,1,773,1-He)[a]	112	103	1.6	4.8

[a] Experiments in which the catalyst was heated in an inert gas. See text for explanation.

As will be discussed later, there are some uncertainties in making a direct comparison between different supports. However, the Ni/Nb_2O_5 catalysts did not undergo a suppression in CO hydrogenation activity, as in ethane hydrogenolysis.

Table 3 shows that the activities of various Ni/Nb_2O_5 catalysts do not differ by more than a factor of 2 to 3; it is thus difficult to identify the effects of crystallite size, reduction temperature, and heating in an inert gas on that basis. A careful examination of all the product distributions, however, identified one characteristic with which different catalysts may be differentiated. This characteristic is the abundance of C_2 hydrocarbons. To illustrate this point the molar ratios of C_2/C_1 for all catalysts at comparable temperatures and conversion levels are shown in Table 4. Such a ratio is around 0.2 for catalysts reduced at 573 K, but more than double its value for catalysts reduced at 773 K. Interestingly enough, the higher temperature itself was insufficient to cause such an effect, as heating the (10, 573, 1) sample in nitrogen to 773 K gave a ratio of 0.166. On the other hand, heating the same sample in helium to 773 K raised the ratio to 0.525. This observation provides yet another piece of evidence that heating in the two inert gases resulted in samples displaying different chemical reactivity.

TABLE 4

Abundance of C_2 Yield in CO Hydrogenation over Ni/Nb_2O_5 Catalysts

Catalyst and treatment	Temperature (K)	CO conversion (%)	Molar ratio of C_2/C_1
(2,573,1)	499	2.6	0.196
(2,773,1)	496	1.3	0.434
(10,573,1)	495	4.1	0.207
(10,773,1)	489	4.0	0.541
(10,573,1,773,1-N_2)[a]	494	2.1	0.166
(10,573,1,773,1-He)[a]	488	2.7	0.525

[a] Experiments in which the catalyst was heated in an inert gas. See text for explanation.

DISCUSSION

Results of Reaction Studies

Our results show that nickel catalysts were less active for ethane hydrogenolysis, but more active for CO hydrogenation when supported on niobia than on silica. Similar trends have been reported for nickel catalysts supported on titania (*4, 10–12*), another SMSI oxide (*22*). As noted previously, our turnover frequencies are calculated using a dispersion based on X-ray diffraction, and not on hydrogen chemisorption which is suppressed on these catalysts (*1*). The uncertainty in quantifying active sites has always been a problem with catalysts which exhibit anomalous chemisorption behavior. Vannice (*28*) showed that the turnover frequency on titania-supported metal catalysts can vary by 1 to 2 orders of magnitude depending on the basis of calculation. Even for a Ni/SiO_2 catalyst, the turnover frequency will be different if the hydrogen uptake on the spent, rather than the fresh catalyst is used (*10*). In the case of CO hydrogenation, the possible loss of activity due to nickel carbonyl formation also needs to be considered (*29*). This is an important point when a comparison is made between different supports, as it has been shown that nickel carbonyl formation is significantly slower on Ni/TiO_2 than on Ni/SiO_2 catalysts (*10*). To ensure a meaningful comparison among catalysts we analyzed our data consistently with the method described. Consequently, it is apparent that our catalysts behaved differently when parameters such as crystallite size, reduction temperature, or reaction conditions were varied, and that the difference is not simply due to the method of calculation.

Aside from activity, our data identify several features characteristic of SMSI. One of them is the change in the experimental rate law for ethane hydrogenolysis, specifically the less negative dependence of the rate on the hydrogen partial pressure. To understand the physical basis of such a change, one needs to examine the mechanism of ethane hydrogenolysis. In the mechanism suggested by Sinfelt (*27*), a less negative value of m corresponds to a less hydrogen-deficient surface species, C_2H_x. This in turn corresponds to a lower dehydrogenation activity relative to the hydrogenolysis activity. Recently, Martin (*30, 31*) proposed an alternative mechanism which allows for the competitive adsorption of methane and hydrogen. This mechanism leads to a different rate law, and a different physical significance of the hydrogen partial pressure dependence. Furthermore, Martin showed that the reaction order with respect to hydrogen partial pressure decreases with increasing temperature on Ni/SiO_2 catalysts. This is a noteworthy point as a catalyst with lower ethane hydrogenolysis activity must be studied at higher temperatures to get an appreciable conversion. Our observed change in the exponent could thus be due to a temperature effect, or to a different surface species as stated above. In any event, our observation that the exponent changed for some catalysts and not for others is significant, as this parameter provides a gauge for the extent of SMSI. We shall return to this point later.

Another interesting manifestation of SMSI in our kinetic results is the unusual selectivity pattern for supported nickel catalysts. The shift in product distributions has been previously found for TiO_2 (*10–12*) and Nb_2O_5 (*32*) supported nickel catalysts

in CO hydrogenation. But these studies did not report an appreciable yield of olefins, as was observed here. In a study with a model supported nickel catalyst, Kao *et al.* (*16*) identified a significant ethylene yield in CO hydrogenation. For the same reaction, Katzer *et al.* (*33*) found that rhodium produces C_2 olefin when supported on titania, but not on silica, and Morris *et al.* (*21*) reported higher propene/propane ratio for Ru/TiO_2 catalysts than for Ru/SiO_2 catalysts. Dalmon and Martin (*34*) suggested that CO hydrogenation can be viewed as a reverse reaction of hydrogenolysis, in the sense that selectivity for higher hydrocarbons (C–C bond formation) increases with decreasing activity for hydrogenolysis (C–C bond rupture). Our data on Ni/Nb_2O_5 catalysts are consistent with this scheme. It is notable that catalysts that produce a large amount of C_2 have the lowest ethane hydrogenolysis activity. Furthermore, the high olefin yields observed in several SMSI systems reflect the low hydrogenation activity of these catalysts. This low activity may be due to the weak binding of hydrogen atoms, as reported by Chen and White (*35*) on TiO_2-supported platinum. Mériaudeau *et al.* (*36*) also found that for titania supported Pt, Ir, and Rh catalysts, hydrogen adsorption capacity and hydrogenation–dehydrogenation activity follow the same trend. It is not surprising that Ni/Nb_2O_5 catalysts which suppress hydrogen adsorption would have low hydrogenation (as shown by higher olefin yields) and dehydrogenation (as shown by a different hydrogen partial pressure dependence in ethane hydrogenolysis) activity.

Interestingly, when nickel is promoted by potassium, the selectivity of CO hydrogenation is shifted to higher hydrocarbons (*37, 38*) and the hydrogenolysis activity decreases (*37*). These effects are usually understood in terms of electron donation from potassium to nickel. Since similar trends have been observed for SMSI catalysts, it is tempting to postulate an analogous transfer of electrons from the support to the metal. Indeed, such a transfer has been suggested by experimental measurement (*15*) and theoretical calculation (*39*). However, one must be cautious in drawing such an analogy. In the case of potassium promotion CO hydrogenation activity actually decreases (*38*); such is not the case for SMSI catalysts. There are thus subtle differences between potassium promotion and SMSI, a point to be discussed in detail later.

A final point to be made about our kinetic results is that they reinforce our earlier conclusions based on hydrogen chemisorption data (*1*). In particular, the experiments involving heating the (10,573,1) sample in an inert gas clearly indicate the different effects due to nitrogen and helium. The use of helium always resulted in a more interacting catalyst. To have a meaningful comparison among the different catalysts as a function of several parameters, a more systematic way of characterizing the extent of SMSI needs to be developed. Such a development is presented in the next section.

Development of a Hierarchy

Results in this study along with those of an earlier report (*1*) for Ni/Nb_2O_5 catalysts identify several manifestations of SMSI behavior in hydrogen chemisorption, ethane hydrogenolysis, and CO hydrogenation. The observation that some of these manifestations occur on certain catalysts but not others suggests that there could be several stages of SMSI. These stages need not be discrete, rather they represent a gradual change in the chemical behavior of a SMSI catalyst as the extent of interaction gets stronger. The strength of the interaction itself depends on parameters such as crystallite size, reduction treatment, and metal/support combination. If a comparison is to be made between different catalysts, then it is desirable to have a system with which the extent of the interaction can be ranked. By comparing results of Ni/Nb_2O_5 and Ni/SiO_2 catalysts, we have established the following criteria on the manifestations of the SMSI behavior:

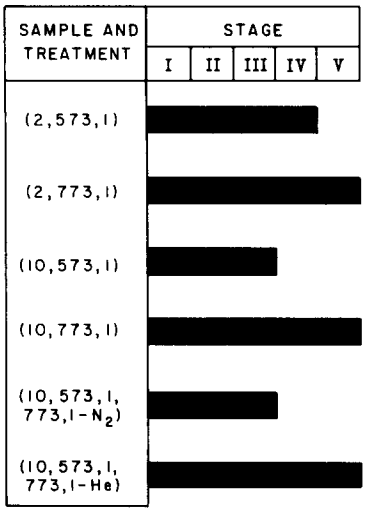

FIG. 2. The extent of strong metal–support interaction for Ni/Nb_2O_5 catalysts as a function of crystallite size, reduction temperature, and inert effect. The stage number corresponds to the number of criteria as explained in the text.

I. A shift in product distribution in CO hydrogenation with comparable or better activity.

II. Lower ethane hydrogenolysis activity.

III. Lower hydrogen chemisorption capability.

IV. A different rate law for ethane hydrogenolysis (reaction order with respect to hydrogen partial pressure changes from ~ -2 to ~ -1).

V. A high C_2 yield in CO hydrogenation.

The above criteria are listed in the order of increasing degree of metal–support interaction. The stage of interaction for a particular catalyst is in turn given by the number of criteria it has met. It should be noted that this ranking system is specifically developed for Ni/Nb_2O_5 catalysts with respect to the three chemical probed used in this study. Its applicability is illustrated in Fig. 2, which clearly shows the effects such as crystallite size and heating in an inert gas on the extent of interaction. Furthermore, Fig. 2 shows that all the niobia-supported nickel catalysts meet the first three criteria, making the separation of these stages suspect. However, it must be remembered that niobia is a very interacting support (*22*), and suppresses hydrogen chemisorption on supported-nickel catalysts even at mild reduction treatments (*1*). Clearly then, to distinguish these stages, evidence must be found on nickel catalysts supported on other less interacting materials. For Ni/TiO_2 catalysts, we previously observed (*7*) that a (10,573,1) sample shows a normal hydrogen chemisorption behavior but a suppression in ethane hydrogenolysis activity. Burch and Flambard (*9*) also reported that for Ni/TiO_2 catalysts, the decline in hydrogen chemisorption is less than the decline in catalytic activity. These observations thus establish the relative positions of criteria II and III. The results of Burch and Flambard (*9*) also help to differentiate the first two criteria. These authors show that a 8.5 wt% Ni/TiO_2 catalyst, after reduction at 723 K, has an ethane hydrogenolysis activity comparable to that of Ni/SiO_2, but is almost 40 times more active in CO/H_2 reaction. The combined data for niobia-supported and titania-supported nickel catalysts thus establish our hierarchy, as proposed.

The idea that there are different stages of SMSI is in itself not a new one, as different authors have found evidence for a more strongly interacting system with increasing reduction temperature (*9, 22*). The advantage of our proposed hierarchy, however, lies in its ability to identify the stage of a particular catalyst with respect to three chemical probes and thus provide a firm basis for comparison among different systems. Due to the many parameters that could affect the extent of interaction in a SMSI catalyst, the hierarchy as a whole also provides a better characterization than the commonly used criterion of hydrogen chemisorption. These points are particularly relevant for comparing results from different laboratories. For example, the Ni/TiO_2 catalyst in the work of Ko and Garten (*4*) is apparently at a more interacting state than those studied by Burch and Flambard (*9*) under mild activation treatments. This

difference could be due to the smaller crystallite size and more severe reduction treatment used in the former study, and could account for the much stronger suppression in ethane hydrogenolysis. In fact, Burch and Flambard (*9*) also observed a strong suppression in ethane hydrogenolysis activity with more severe reduction conditions. Unfortunately we cannot apply our full hierarchy to their more severely reduced samples, as these authors did not report any corresponding hydrogen chemisorption data, nor an experimental rate law for ethane hydrogenolysis.

Mechanism of SMSI

As mentioned above, the various stages of SMSI correspond to a gradual, rather than discrete, change in catalyst behavior as the extent of interaction gets stronger. It has been well established that reduction of the support is a necessary step for SMSI behavior (*40*). Tauster and Fung (*22*) first noted an empirical correlation between the extent of SMSI and oxide reducibility for supported iridium catalysts. A qualitatively similar trend was reported in our previous work (*1*) on titania-supported versus niobia-supported nickel catalysts.

The sequence of events following the reduction of the support remains a matter of debate. The work of Kao *et al.* (*15, 16*) shows that for a model supported nickel catalyst, there is a charge transfer from the support to the metal. If electron transfer is indeed a prevailing mechanism for SMSI, then it is of interest to compare the chemical properties of our catalysts with those of potassium-promoted nickel catalysts, as the promoting effect of potassium is believed to be associated with electron donation as well (*38*). Such a comparison reveals some similarities. Potassium promotion on nickel has been shown to decrease ethane hydrogenolysis activity (*37, 41, 42*), and shift the product distribution of CO/H_2 reaction to higher hydrocarbons (*37, 38*). Similar trends were found in this study for Ni/Nb_2O_5 catalysts. However, the decrease in ethane hydrogenolysis for our catalysts (a factor of about 10^2–10^3) is significantly larger than that found for potassium promotion (less than a factor of 50) (*41, 42*). Perhaps more disturbing is the fact that potassium promotion decreases the activities of both ethane hydrogenolysis and CO/H_2 reaction (*37, 41, 42*), whereas the activities for the same two reactions are affected in different directions for SMSI catalysts. Thus it is apparent that electron transfer may play a role in SMSI, but by itself cannot adequately explain our observations.

The inadequacy of a simple electron transfer argument suggests the presence of some type of geometric effect. Recently, convincing arguments have been put forth by Santos *et al.* (*43*) for Fe/TiO_2 and Resasco and Haller (*44*) for Rh/TiO_2 catalysts that there is a migration of the reduced oxide onto the metal particle. Results in this study are also consistent with the presence of such oxide species on the metal surface. For example, these species can lower ethane hydrogenolysis activity through a simple geometric effect of diluting active nickel ensembles. Sinfelt *et al.* (*45*) reported a very significant decrease in ethane hydrogenolysis activity with increasing Cu concentration in a series of copper–nickel alloys, and the analogy between the dilution effect due to copper and that due to oxide migration was first emphasized by Resasco and Haller (*44*). It should be noted that in the unsupported Cu–Ni catalysts used by Sinfelt *et al.*, the surface copper concentration is very high even at a low bulk copper concentration, due to the preferential segregation of copper to the surface (*46*). The recent work of Dalmon and Martin (*47*), who used supported Ni–Cu alloys with similar surface and bulk compositions provides an alternate basis of comparison. These authors also observed a significant, but less gradual drop in ethane hydrogenolysis activity of these supported Ni–Cu alloys as the copper content increases. Such an observation is fully accounted for by a purely

geometric effect of dilution. Interestingly, the hydrogen partial pressure dependence in the rate law remains the same (~ -2) in this series of catalysts, despite the drop in activity.

The above evidence shows that neither electron transfer nor dilution effects alone can satisfactorily explain our data. We are thus led to believe that, similar to the conclusions of Resasco and Haller (*44*), electronic and geometric effects are working in concert on our Ni/Nb_2O_5 catalysts. The idea of the surface being covered by migrating oxide species is particularly appealing in that it provides a possible reason for the different behavior of the two probe reactions. Although the presence of migrating species decreases the ethane hydrogenolysis activity, the activity for CO hydrogenation will not be adversely affected if special active sites exist at the interface between the metal surface and these species. It is necessary to invoke these active sites as from a pure geometric viewpoint, the presence of migrating oxide should decrease the CO hydrogenation activity due to a diluting effect similar to that observed for Ni–Cu alloy films (*48*), and such was not the case for Ni/Nb_2O_5 catalysts. Burch and Flambard (*8, 9*) have postulated new active sites for CO hydrogenation at the metal–support interface. We suggest that these sites are not limited to the contact area between the metal crystallite and the support, rather they are distributed over the crystallite surface. Recall that the samples used by Burch and Flambard are at an early stage of interaction (no significant suppression in ethane hydrogenolysis activity). It is probable that at this stage the migration process has not occurred to an appreciable extent, consequently special sites associated with metal-reduced oxide interface will be limited to the periphery of the crystallite. The argument above is supported by the work of Chung *et al.* (*49*), who found similar catalytic behavior between $TiO_x/Ni(111)$ and $Ni/TiO_2(100)$ samples in CO hydrogenation.

Recently several investigators have published electron microscopy results which show a structural change of the supported metal crystallites in several SMSI systems. Pillbox, or raftlike, structures are found for Pt (*50, 51*), Ni (*52*), and Ag (*53*) supported on various oxides of titanium. In this study we have no direct evidence for a structural change of the nickel crystallites. On the other hand, the possible occurrence of such a process is not inconsistent with our chemical observations. For example, the manifestations of Stages IV and V in our more interacting catalysts could be related to a morphological change. The fact that a more severe reduction treatment was necessary to get a catalyst into these later stages suggests that for these samples, the migrating oxide concentration on the crystallite surface was higher. Perhaps a critical oxide coverage is associated with a morphological change.

The mechanism of SMSI discussed thus far not only forms a physical basis for our hierarchy, but also provides insights into the parameters which have been found to be important for Ni/Nb_2O_5 catalysts (*1*). This mechanism is consistent with the facts that SMSI affects the smaller crystallite more at a given reduction temperature, and becomes more severe with increasing reduction treatment. When a comparison is made between TiO_2 and Nb_2O_5 supports, the more interacting behavior of the latter can be accounted for by its higher reducibility in addition to its lower melting point which would facilitate migration. Finally, the difference between heating a (10,573,1) sample in nitrogen versus helium can also be explained. Nitrogen adsorption on TiO_2-supported Rh (*54*) and Ni (*55*) catalysts has been reported. Nitrogen adsorption on the metal–support interface can hinder the migration of the reduced species, resulting in a less interacting catalyst compared to the one heated in helium.

Our model shares many common features with those suggested by Santos *et al.* (*43*) and Resasco and Haller (*44*). These similarities suggest the same mechanism for

TiO_2 and Nb_2O_5 as SMSI supports. However, there appears to be a subtle difference when different metals are supported on these oxides. In particular the direction of electron transfer seems to be different between Ni and Fe (*43*). Vannice (*28*) also pointed out that the effects of SMSI on CO hydrogenation vary markedly among Group VIII transition metals. We thus want to emphasize again that our hierarchy and model are developed specifically for supported nickel catalysts. The application of this hierarchy to other metal/support combinations, or the development of similar ranking systems on the basis of additional chemical probes, will hopefully further elucidate the nature of SMSI.

SUMMARY

Niobia-supported nickel catalysts have been shown to exhibit chemical behavior different from that of silica-supported nickel catalysts in ethane hydrogenolysis and CO hydrogenation. For these catalysts the activity for ethane hydrogenolysis is lower, and the experimental rate law is different for the more severely reduced samples. In the case of CO hydrogenation, the activity is not adversely affected but the product distribution shifts to higher hydrocarbons that contain a significant amount of olefins. These observations are attributed to strong metal–support interaction (SMSI). SMSI is found to be stronger for the catalyst with a smaller crystallite size at the same reduction temperature, or with increasing reduction temperatures for the same catalyst.

The use of hydrogen chemisorption, ethane hydrogenolysis, and CO hydrogenation has identified different manifestations of SMSI. A particular catalyst may show any number of these manifestations depending on the support, the crystallite size, and the reduction treatment. These observations suggest that there are different stages of SMSI, and lead to the development of a hierarchy with which the extent of interaction for SMSI catalysts can be systematically ranked and compared. To provide a physical basis for this hierarchy, a mechanism of SMSI that involves the reduction of the support and the subsequent migration of the reduced oxide onto the metal surface is proposed.

ACKNOWLEDGMENTS

Acknowledgment is made to the Donors of the Petroleum Research Fund, administered by the American Chemical Society, for partial support of this research. We also thank Sun Company and Air Products and Chemicals, Inc. for their equipment grants which facilitated this work.

REFERENCES

1. Ko, E. I., Hupp, J. M., Rogan, F. H., and Wagner, N. J., *J. Catal.* **84,** 85 (1983).
2. Tauster, S. J., Fung, S. C., and Garten, R. L., *J. Amer. Chem. Soc.* **100,** 170 (1978).
3. Ko, E. I., Hupp, J. M., and Wagner, N. J., *J. Chem. Soc. Chem. Commun.* 94 (1983).
4. Ko, E. I., and Garten, R. L., *J. Catal.* **68,** 233 (1981).
5. Haller, G. L., Resasco, D. E., and Rouco, A. J., *Faraday Discuss. Chem. Soc.* **72,** 109 (1981).
6. Resasco, D. E., and Haller, G. L., *in* "Studies in Surface Science and Catalysis" (B. Imelik *et al.*, Eds.), Vol. 11, p. 43. Elsevier, Amsterdam/New York, 1982.
7. Ko, E. I., Winston, S., and Woo, C., *J. Chem. Soc. Chem. Commun.* 740 (1982).
8. Burch, R., and Flambard, A. R., *in* "Studies in Surface Science and Catalysis" (B. Imelik *et al.*, Eds.), Vol. 11, p. 193. Elsevier, Amsterdam/New York, 1982.
9. Burch, R., and Flambard, A. R., *J. Catal.* **78,** 389 (1982).
10. Vannice, M. A., and Garten, R. L., *J. Catal.* **56,** 236 (1979).
11. Vannice, M. A., and Garten, R. L., *J. Catal.* **66,** 242 (1980).
12. Bartholomew, C. H., Pannell, R. B., and Butler, J. L., *J. Catal.* **65,** 335 (1980).
13. Turlier, P., Dalmon, J. A., and Martin, G. A., *in* "Studies in Surface Science and Catalysis" (B. Imelik *et al.*, Eds.), Vol. 11, p. 203. Elsevier, Amsterdam/New York, 1982.
14. Vannice, M. A., and Vasco-Jara, J., *in* "Studies in Surface Science and Catalysis" (B. Imelik *et al.*, Eds.), Vol. 11, p. 185. Elsevier, Amsterdam/New York, 1982.
15. Kao, C. C., Tsai, S. C., Bahl, M. K., and Chung, Y. W., *Surf. Sci.* **95,** 1 (1980).
16. Kao, C. C., Tsai, S. C., Bahl, M. K., and Chung, Y. W., *J. Catal.* **73,** 136 (1982).

17. Kao, C. C., Tsai, S. C., and Chung, Y. W., *in* "Studies in Surface Science and Catalysis" (B. Imelik *et al.*, Eds.), Vol. 11, p. 211. Elsevier, Amsterdam/New York, 1982.
18. Vannice, M. A., Twu, C. C., and Moon, S. H., *J. Catal.* **79,** 70 (1983).
19. Vannice, M. A., Wang, S. Y., and Moon, S. H., *J. Catal.* **71,** 152 (1981).
20. Wang, S. Y., Moon, S. H., and Vannice, M. A., *J. Catal.* **71,** 167 (1981).
21. Morris, S. R., Moyes, R. B., and Wells, P. B., *in* "Studies in Surface Science and Catalysis" (B. Imelik *et al.*, Eds.), Vol. 11, p. 247. Elsevier, Amsterdam/New York, 1982.
22. Tauster, S. J., and Fung, S. C., *J. Catal.* **54,** 29 (1978).
23. Phadke, M. D., M.S. thesis, Carnegie–Mellon Univ., Pittsburgh, Pa., 1982.
24. Yates, D. J. C., Taylor, W. F., and Sinfelt, J. H., *J. Amer. Chem. Soc.* **86,** 2996 (1964).
25. Vannice, M. A., *J. Catal.* **37,** 449 (1975).
26. Taylor, W. F., Sinfelt, J. H., and Yates, D. J. C., *J. Phys. Chem.* **69,** 3857 (1965).
27. Sinfelt, J. H., *Catal. Rev.* **3,** 175 (1969).
28. Vannice, M. A., *J. Catal.* **74,** 199 (1982).
29. Shen, W. M., Dumesic, J. A., and Hill, G. C., Jr., *J. Catal.* **68,** 152 (1981).
30. Martin, G. A., *J. Catal.* **60,** 345 (1979).
31. Martin, G. A., *J. Catal.* **60,** 452 (1979).
32. Kugler, E. L., and Tauster, S. J., U.S. Patent 4,206,135 (1980).
33. Katzer, J. R., Sleight, A. W., Gajardo, P., Michel, J. B., Gleason, E. F., and McMillan, S., *Faraday Discuss. Chem. Soc.* **72,** 121 (1981).
34. Dalmon, J. A., and Martin, G. A., *in* "Studies in Surface Science and Catalysis" (T. Seiyama and K. Tanabe, Eds.), Vol. 7, p. 402. Elsevier, Amsterdam/New York, 1981.
35. Chen, B.-H., and White, J. M., *J. Phys. Chem.* **86,** 3534 (1982).
36. Mériaudeau, P., Ellestad, O. H., Dufaux, M., and Naccache, C., *J. Catal.* **75,** 243 (1982).
37. Martin, G. A., *in* "Studies in Surface Science and Catalysis" (B. Imelik *et al.*, Eds.), Vol. 11, p. 315. Elsevier, Amsterdam/New York, 1982.
38. Campbell, C. T., and Goodman, D. W., *Surf. Sci.* **123,** 413 (1982).
39. Horsley, J. A., *J. Amer. Chem. Soc.* **101,** 2870 (1979).
40. Tauster, S. J., Fung, S. C., Baker, R. T. K., and Horsley, J. A., *Science* **211,** 1121 (1981).
41. Praliaud, H., Dalmon, J. A., Martin, G., Primet, M., and Imelik, B., *C. R. Acad. Sci. Ser. C* **291,** 89 (1980).
42. Rostrup-Nielsen, J. R., *J. Catal.* **31,** 173 (1973).
43. Santos, J., Phillips, J., and Dumesic, J. A., *J. Catal.* **81,** 147 (1983).
44. Resasco, D. E., and Haller, G. L., *J. Catal.* **82,** 279 (1983).
45. Sinfelt, J. H., Carter, J. L., and Yates, D. J. C., *J. Catal.* **24,** 283 (1972).
46. Burton, J. J., and Hyman, E., *J. Catal.* **37,** 114 (1975).
47. Dalmon, J. A., and Martin, G. A., *J. Catal.* **66,** 214 (1980).
48. Ponec, V., *Catal. Rev.-Sci. Eng.* **18**(1), 151 (1978).
49. Chung, Y. W., Xiong, G., and Kao, C. C., *J. Catal.* **85,** 237 (1984).
50. Baker, R. T. K., Prestridge, E. B., and Garten, R. L., *J. Catal.* **59,** 293 (1979).
51. Chen, B.-H., White, J. M., Brostrom, L. R., and Deviney, M. L., *J. Phys. Chem.* **87,** 2423 (1983).
52. Smith, J. S., Thrower, P. A., and Vannice, M. A., *J. Catal.* **68,** 270 (1981).
53. Baker, R. T. K., Prestridge, E. B., and Murrell, L. L., *J. Catal.* **79,** 348 (1983).
54. Resasco, D., and Haller, G. L., *J. Chem. Soc., Chem. Commun.* 1150 (1980).
55. Burch, R., and Flambard, A. R., *J. Chem. Soc., Chem. Commun.* 965 (1981).